(2)

AD-A186 810

REPORT DOCUMENTATION PAGE

1b RESTRICTIVE MARKINGS	
2a SECURITY CLASSIFICATION AUTHORITY	3 DISTRIBUTION/AVAILABILITY OF REPORT: Approved for public release; distribution unlimited.
2b DECLASSIFICATION/DOWNGRADING SCHEDULE	
4 PERFORMING ORGANIZATION REPORT NUMBER(S)	5 MONITORING ORGANIZATION REPORT NUMBER(S): ARO 21490.19-MS
6a NAME OF PERFORMING ORGANIZATION: Wayne State University	6b OFFICE SYMBOL (If applicable):
7a NAME OF MONITORING ORGANIZATION: U. S. Army Research Office	
6c ADDRESS (City, State, and ZIP Code): Detroit, MI 48202	7b ADDRESS (City, State, and ZIP Code): P. O. Box 12211, Research Triangle Park, NC 27709-2211
8a NAME OF FUNDING/SPONSORING ORGANIZATION: U. S. Army Research Office	8b OFFICE SYMBOL (If applicable):
9 PROCUREMENT INSTRUMENT IDENTIFICATION NUMBER	
8c ADDRESS (City, State, and ZIP Code): P. O. Box 12211, Research Triangle Park, NC 27709-2211	10 SOURCE OF FUNDING NUMBERS: PROGRAM ELEMENT NO; PROJECT NO; TASK NO; WORK UNIT ACCESSION NO

11 TITLE (Include Security Classification): Thermal Wave Imaging (Unclassified)

12 PERSONAL AUTHOR(S): R.L. Thomas, L.D. Favro, and P.K. Kuo

13a TYPE OF REPORT	13b TIME COVERED	14 DATE OF REPORT (Year, Month, Day)	15 PAGE COUNT
Final	FROM 8/15/84 TO 9/30/87	1987, October, 30	31

16 SUPPLEMENTARY NOTATION: The view, opinions and/or findings contained in this report are those of the author(s) and should not be construed as an official Department of the Army position, policy, or decision, unless so designated by other documentation.

17 COSATI CODES		
FIELD	GROUP	SUB-GROUP

18 SUBJECT TERMS (Continue on reverse if necessary and identify by block number): Thermal Wave Imaging, Nondestructive evaluation, Materials characterization

19 ABSTRACT (Continue on reverse if necessary and identify by block number)

Several aspects of thermal wave techniques for imaging defects and characterizing material properties have been studied during the course of this contract. Among the thermal wave detection techniques which were investigated are the mirage-effect (optical probe beam), the thermoacoustic effect, photothermal reflectance, and infrared (IR) video lock-in imaging. Both experiment and theory have been studied, and applications made to crack-detection, layered structures and delaminations, semiconductor devices, and contactless measurements of thermal diffusivities.

20 DISTRIBUTION/AVAILABILITY OF ABSTRACT	21 ABSTRACT SECURITY CLASSIFICATION	
☐ UNCLASSIFIED/UNLIMITED ☐ SAME AS RPT ☐ DTIC USERS	Unclassified	
22a NAME OF RESPONSIBLE INDIVIDUAL	22b TELEPHONE (Include Area Code)	22c OFFICE SYMBOL

DD FORM 1473, 84 MAR — 83 APR edition may be used until exhausted. All other editions are obsolete.

SECURITY CLASSIFICATION OF THIS PAGE: UNCLASSIFIED

ARO 21490.19-MS

THERMAL WAVE IMAGING

FINAL REPORT

R.L. Thomas, L.D. Favro and P.K. Kuo

October 30, 1987

CONTRACT NUMBER DAAG29-84-K-0173

WAYNE STATE UNIVERSITY

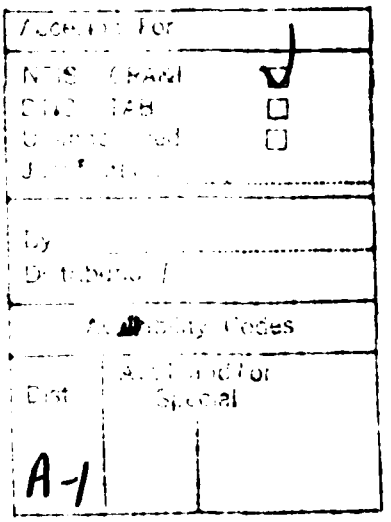

THE VIEWS, OPINIONS, AND/OR FINDINGS CONTAINED IN THIS REPORT ARE THOSE OF THE AUTHORS AND SHOULD NOT BE CONSTRUED AS AN OFFICIAL DEPARTMENT OF THE ARMY POSITION, POLICY, OR DECISION, UNLESS SO DESIGNATED BY OTHER DOCUMENTATION.

FOREWORD

Several aspects of thermal wave techniques for imaging defects and characterizing material properties have been studied during the course of this contract. Among the thermal wave detection techniques which were investigated are the mirage-effect (optical probe beam), the thermoacoustic effect, photothermal reflectance, and infrared (IR) video lock-in imaging. Both experiment and theory have been studied, and applications made to crack-detection, layered structures and delaminations, semiconductor devices, and contactless measurements of thermal diffusivities.

TABLE OF CONTENTS

LIST OF ILLUSTRATIONS

LIST OF ILLUSTRATIONS (Continued)

A. STATEMENT OF THE PROBLEM STUDIED

A three year program of research was carried out to develop several thermal wave imaging techniques and to explore applications of those techniques to NDE of semiconductors, metal alloys and composite materials. Both experimental and theoretical studies were conducted. The ultimate goal of the research program was the development of thermal wave techniques for nondestructive evaluation (NDE) and materials characterization applications. A general objective essential to the achievement of that goal was the establishment of a firm experimental and theoretical scientific basis for each of the thermal wave imaging schemes studied as they pertain to the detection of scattering of thermal waves from typical subsurface structures and defects. Some of the specific objectives identified in the research proposal were:

1. The basic study of mirage effect and photothermal reflectance detection of thermal wave scattering from subsurface structures and defects, both experiment and theory.
2. Study of the photothermal deflection technique in the time domain, experiment and theory.
3. Instrumental development of each of the techniques available with the objectives of extending the frequency range, improving the signal/noise ratio, the resolution, the scanning routines and the data processing.
4. Comparison of the various techniques for application to the study of several classes of materials, including (1) semiconductors, with an objective to assess the capability of detecting and characterizing layer defects with high resolution; (2) metal alloys, with an objective to assess the comparative capability of the different detection methods for imaging grain boundaries and other metallurgical characteristics; (3) carbon-carbon composite materials, to determine the feasibility of distinguishing cracks from the intrinsic heterogeneity; of the material
5. Exploratory investigation of the capability of the technique as a materials characterization technique, specifically for the measurement of variations in <u>local</u> thermal parameters for intermediate state superconductors, and for phase transitions in superconductors and in selected magnetic materials.

During the contract period, the principal investigators were also awarded an ARO Instrumentation Grant [Contract Number DAAL 03-86-G-0169, 7/7/86-7/6/87] , "Instrumentation for Thermal Wave Imaging." The resulting instrumentation which we developed in this laboratory was used to demonstrate some of the practical advantages of carrying out thermal wave imaging with the use of infrared (IR) video camera techniques, coupled with various synchronous heating schemes and our newly developed image processing hardware and software. This instrumentation was applied to the problems listed above, and others which emerged during the course of the research.

B. SUMMARY OF THE MOST IMPORTANT RESULTS

Mirage-effect thermal wave detection and imaging of brittle fracture cracks

Figure 1 shows a comparison between scanned optical images and mirage effect thermal wave images of brittle fracture cracks induced in a SiC ceramic by means of diamond tip (Knoop) indentations [R.L. Thomas, L.D. Favro, P.K. Kuo, D.N. Rose, D.C. Bryck, M. Chaika, and J. Patt, *U.S. Army TACOM Technical Report No. 13077*, July 1985]. The specimens were provided by Robert Brokelman of the Army Materials and Mechanics Research Center. The original surface indentations had been previously ground away, rendering the cracks optically invisible, yet still easily detectable by thermal wave imaging.

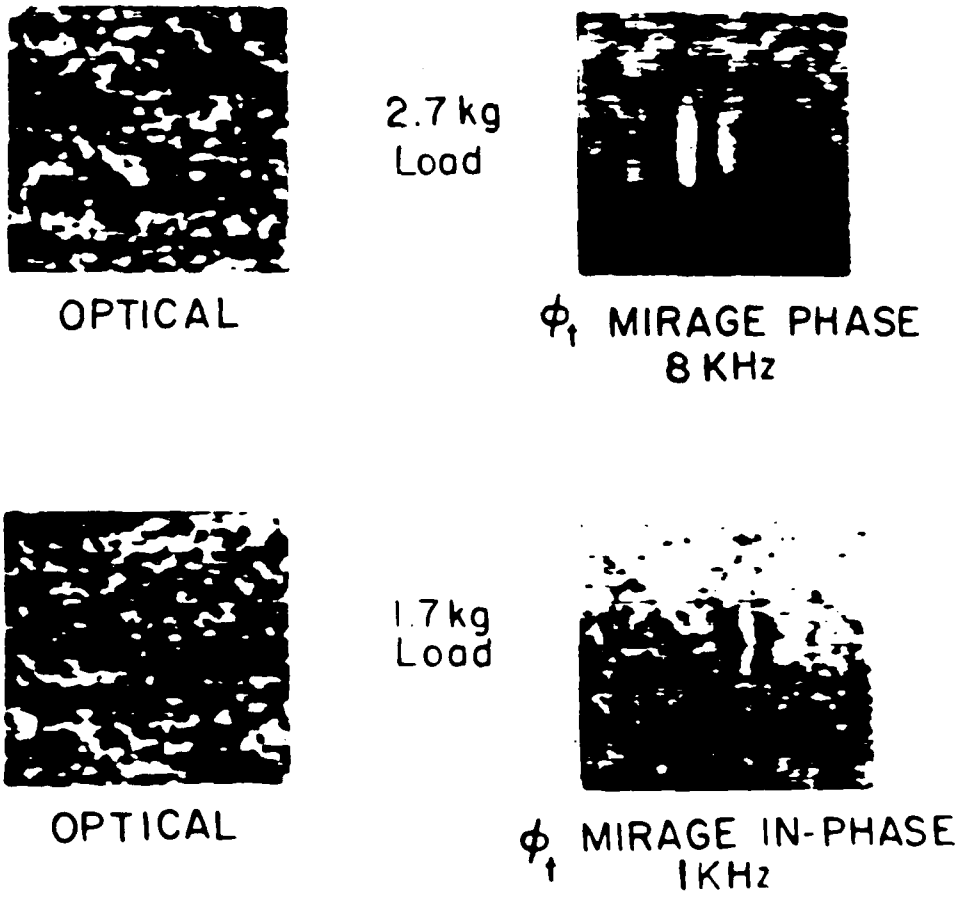

Fig. 1 Comparison of scanned optical and thermal wave images of brittle fracture cracks in SiC ceramic material

Thermal wave material characterization: measurements of thermal diffusivity

The mirage effect detection scheme can also be used as a means of characterizing materials through the determination of thermal diffusivity, a combination of the thermal conductivity and heat capacity. Essentially the technique consists of a direct measurement of the thermal wavelength together with the frequency [P.K. Kuo, L.D. Favro, and R.L. Thomas, in *Photothermal Spectroscopy*, Jeffrey A. Sell, ed., Academic Press (to be published)]. The technique is totally contactless, only requires access to one side of the specimen, and can be performed locally in regions of the order of 1 mm in size. The technique benefits quantitatively from the excellent agreement which we have achieved between our detailed theory and experimental data. Figures 2 and 3 illustrate the agreement between the experimental and theoretical waveforms for the case of the element chromium. This is further illustrated in Fig. 4, in which thermal wavelengths have been determined for chromium over a wide range of frequencies and plotted ("crossing") versus the inverse root frequency. In this plot, the points are experimental determinations, and the curve the theoretical predictions for chromium.

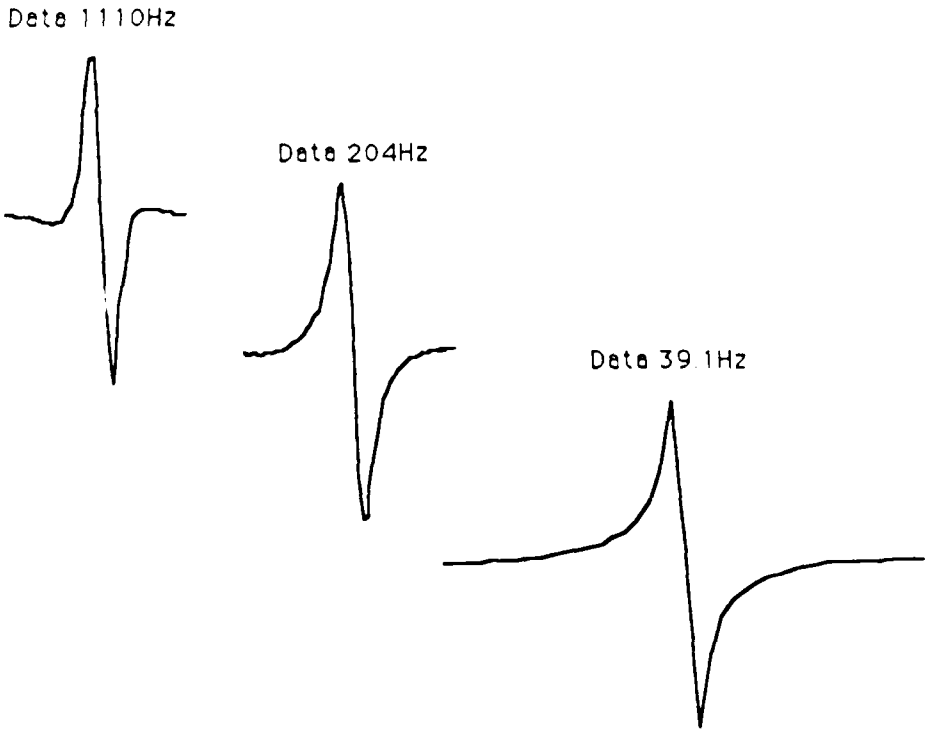

Fig. 2 Experimental waveform (diffusivity measurement) for chromium

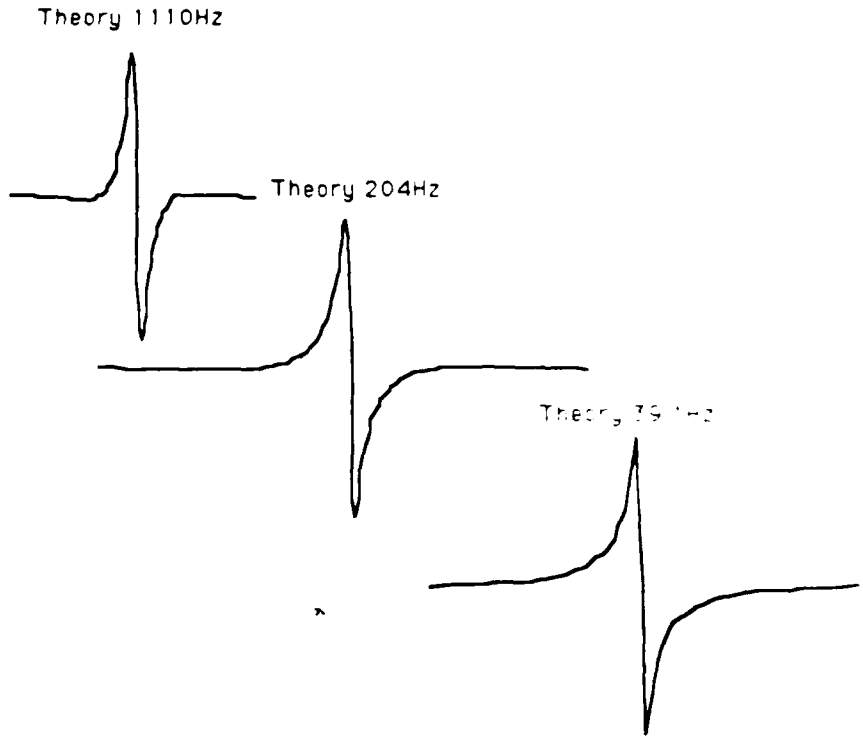

Fig. 3 Theoretical waveform (diffusivity measurement) for chromium

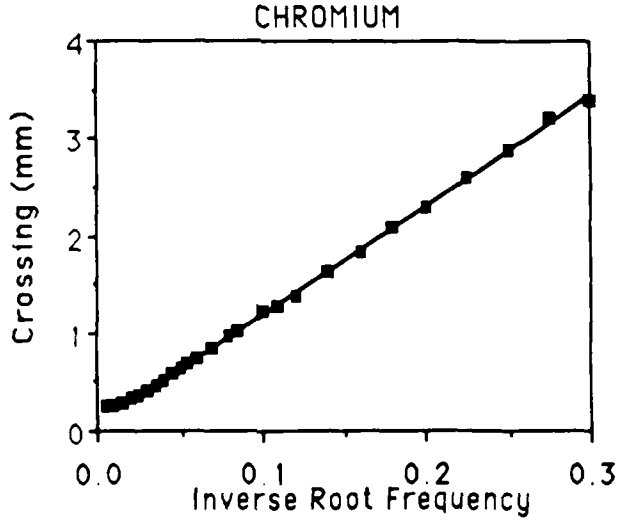

Fig. 4 Frequency-dependence of wavelength (theory,line; expt.,points) for Cr

In order to test the accuracy of this technique, we have determined the diffusivities of a variety of

elements in the periodic table, and the results of our measurements are compared to handbook values in Fig. 5 below. The excellent agreement gives us confidence that the method can be applied to materials of practical interest with a wide range of diffusivities.

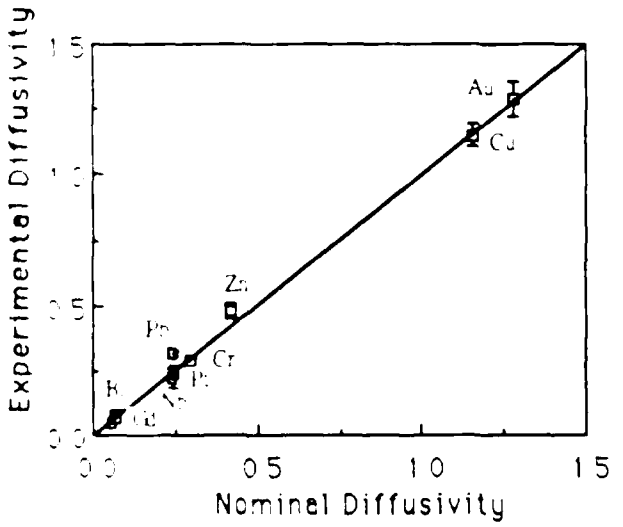

Fig. 5 Comparison of thermal wave determinations of diffusivity with handbook values for pure elemental solids

Mirage-effect characterization of coatings

We have extended our theory originally developed for the diffusivity measurement to include layered structures, so that the experiment can be extended to the study of coatings and films. Figure 6 shows the good agreement we have obtained between theory (curves) and experiment (points) for thin films of copper on glass. This agreement provides the basis for a technique to measure thicknesses of very thin films.

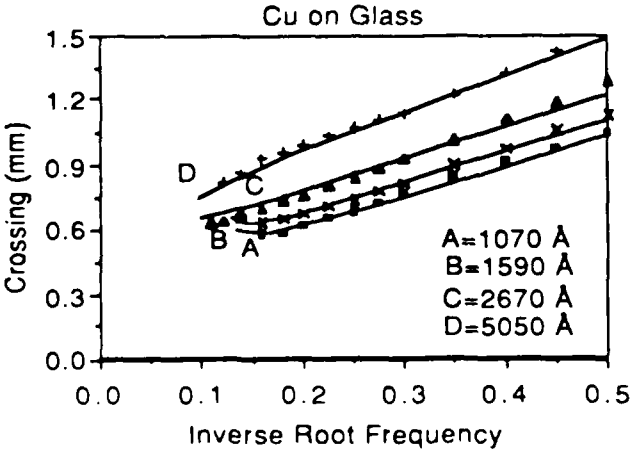

Fig. 6 Theory (lines); experiment (points) for Cu films on glass

Mirage-effect imaging of semiconductor devices

Figure 7 shows an ordinary optical microscope image, a scanned optical image, and a mirage-effect thermal wave image of a semiconductor test pattern on a multilevel metallization structure (Al on polyimide on Al on SiO_2 on Si) [R.L. Thomas and A. Rosencwaig, *Review of Progress in Quantitative NDE*, Eds. D.O. Thompson and D. E. Chimenti, Plenum, 1985, Vol. 4B, pp. 1177-1188] It may be noted that the stitch pattern on the left, which is partially on the surface and partially underneath, is discontinuous in both of the optical images, which only show surface features. The thermal wave image, on the other hand, shows the continuity of the pattern, because of its ability to see beneath the surface.

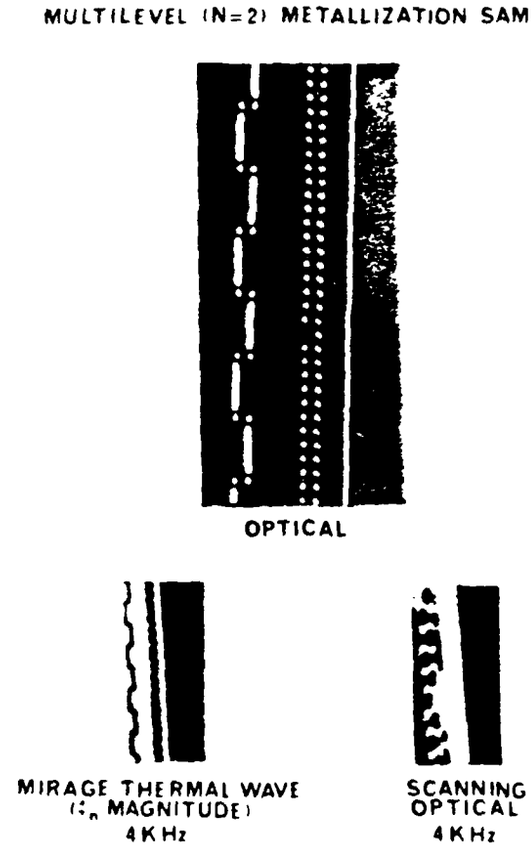

Fig. 7 Comparison between optical and thermal wave images of a multilevel metallization sample (Al on polyimide on Al on SiO_2 on Si)

Thermal wave IR imaging of layered structures

Probably the most important thermal wave imaging techniques from the practical point of view are the ones which we are currently developing by employing a commercial IR video camera, coupled to a high-speed, on-line video processor, and using our novel image processing algorithms and hardware. The importance of these techniques lies in their vastly improved image acquisition speeds, which are fast enough for use on the factory floor. They are also more robust, and do not need the elaborate vibration isolation required by some of the previous methods.

Time-Resolved IR Video Imaging with Synchronized Scanned Laser Heating[†]

Recent advances in the speed and sensitivity of cooled HgCdTe detectors have made it possible to construct an infrared video camera with a single detector by using mirror scanning techniques. The commercial availability of this kind of camera has led to interesting techniques for thermal wave imaging. For example, they have been used with flash lamps for imaging defects in materials [1], and with a scanned IR source for measuring thermal diffusivities [2,3]. With an infrared camera, vast amounts of thermal information from an entire area can be gathered in parallel. This method has obvious advantages in imaging as compared to the more traditional methods of acoustic detection, optical beam deflection or focused (unscanned) IR detection, each of which require a slow scan of the sample to obtain an image. The infrared video camera alone, due to its fixed rate of 50 or 60 fields per second, cannot catch fast thermal phenomena (in the millisecond range). The method described here, which uses the video camera in combination with a focused and scanned optical laser beam, synchronized with the camera's vertical scan, circumvents that limitation. It is capable of observing thermal phenomena on a sub-millisecond time scale and also can acquire data on an entire vertically scanned line at the video field rate. As such, it is useful for studying coatings and thin films, even with thicknesses down to the sub-micron range, and is fast enough for many potential process control and NDE applications.

A block diagram of the instrumentation is shown in Fig. 8. The instrument uses an Ar-ion laser, an A/O modulator for beam blanking during retrace, and a microcomputer-controlled mirror scanning system which is synchronized with the vertical scanning of the video camera (Inframetrics Model IR-600 operated in the 8-12 μm band, either with a 1.8 inch focal length microscope objective or a 6

[†]P.K. Kuo, I.C. Oppenheim, L.D. Favro, Z.J. Feng, R.L. Thomas, J. Hartikainen and L.J. Inglehart, Proc. 5th International Topical Meeting on Photoacoustic and Photothermal Phenomena, Springer-Verlag, Heidelberg (to be published).

inch close-up lens). A second microcomputer is used for image processing. For time scales of 0.1 ms or longer, the video camera's horizontal scan time (64 μs) is fast enough to be considered as being instantaneous. Thus, the video camera can be considered as providing a moving line of point detectors, gathering data in parallel.

The mirror scanning system is programmed to keep the focused laser beam a fixed temporal interval ahead of the moving line of detectors. The fixed temporal advance can be programmably controlled to better than 0.1 ms accuracy. This arrangement improves the effective detection bandwidth of the infrared camera to 16 kHz (the horizontal scan rate). The spatial resolution is limited by the size of the focused laser beam and not by the camera's IR detector [4], and thus could be as small as 1μm. The focused source, coupled with spatially distributed point detectors, provides the opportunity to measure lateral heat flow. This capability turns out to be very advantageous when applied to thin (submicron) film structures.

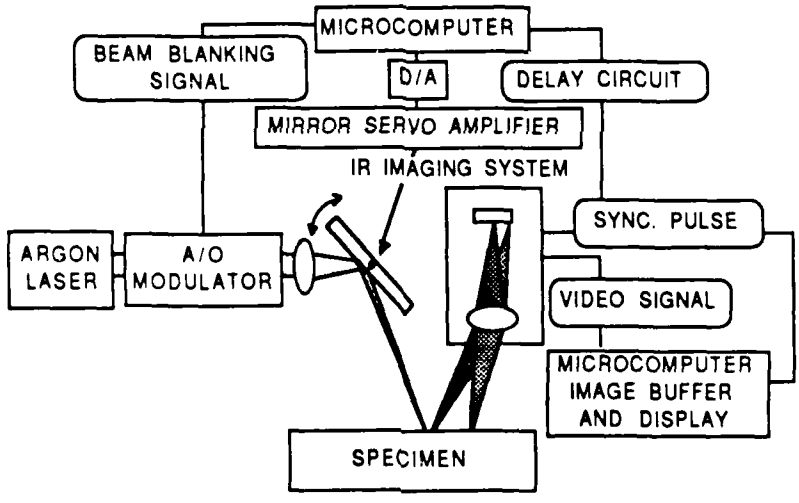

Fig. 8

Block diagram of imaging system.

The technique described here is capable of detecting the presence of very thin films, as well as delaminations between films by exploiting the behavior of three-dimensional heat flow. Here, we give an example in which a 0.1 μm boron film is detected underneath a 0.6 μm ZrN film on a silicon substrate (Figs. 9 and 10). Figure 9 shows a schematic diagram, and Fig. 10 an IR image of the 0.1 μm film of boron deposited underneath a 0.6 μm film of ZrN on a silicon substrate, obtained with this

instrument. This image was taken in reflection, using the 6 inch IR close-up lens, and clearly indicates the presence of the subsurface boron film through its influence on the short-time-scale transverse heat flow. The boron film is undetectable optically, and also cannot be seen using conventional IR thermography.

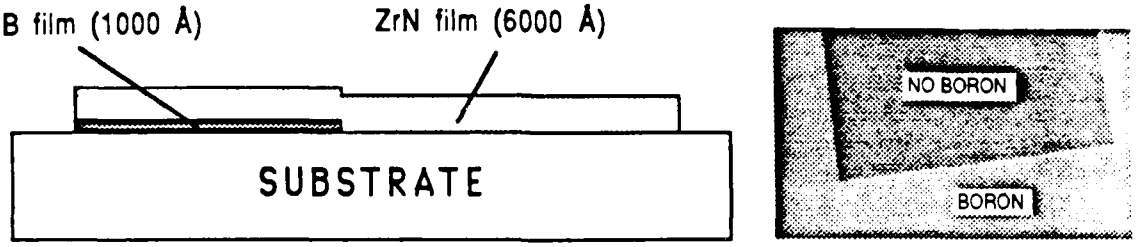

Fig 9 Schematic diagram (left) of ZrN/B/Silicon sample whose scanned IR thermal wave image is shown in Fig. 10. Schematic diagram of boron film location and shape (right).

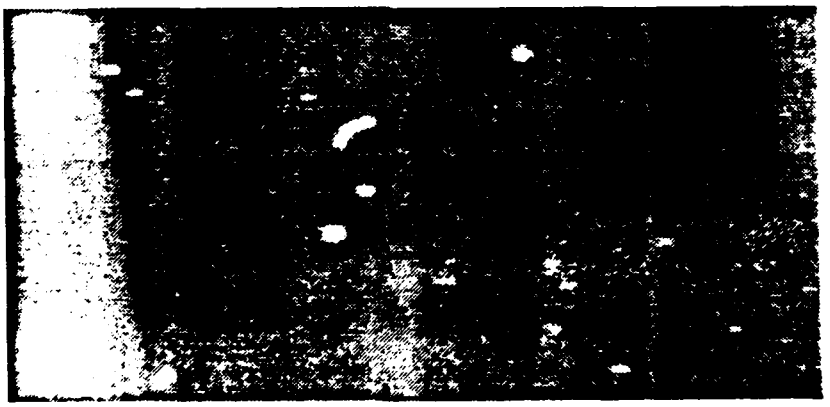

Fig. 10 Scanned IR thermal wave image of the ZrN/B/Silicon sample shown schematically in Fig. 9. The dark (hotter) region is a region under which the B film is present.

As noted above, the technique is sensitive to defects in thin film structures. To illustrate this sensitivity, in Fig. 11 we show an image of a 0.1 μm film of boron on a glass substrate, obtained with this instrument. This image was taken in reflection, using the 6 inch IR close-up lens. The image covers a 1.5 mm x 6.5 mm region of the film which contains extensive delaminated regions which are clearly apparent in the thermal wave image.

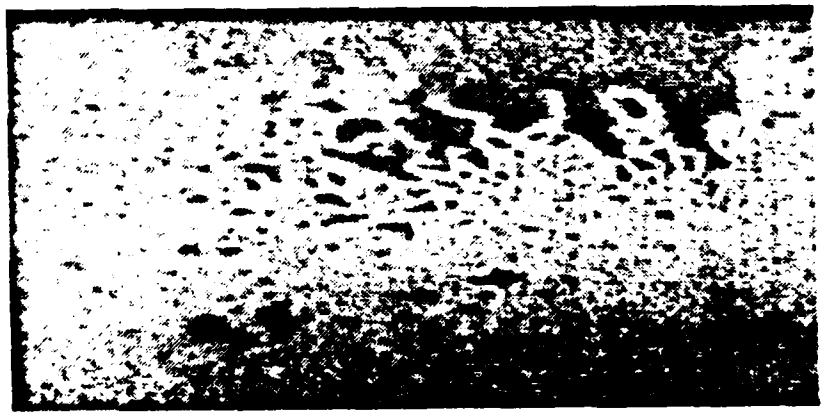

Fig. 11 IR image of a 0.1 μm film of boron on a glass substrate, obtained with this instrument. This image was taken in reflection, using the 6 inch IR close-up lens. The image covers a 1.5 mm x 6.5 mm region of the film which contains extensive delaminated (dark/hotter) regions.

delaminated (dark/hotter) regions.

Thermal Wave Imaging Using an Area-Wide Vector Lock-In Video Technique[‡]

In conventional scanned thermal wave imaging, a lock-in analyzer synchronized to the source of the thermal wave is used to improve the ratio of signal to noise. Such techniques suffer the practical disadvantage of slow speed, since data are taken point-by-point, with each point requiring a few tens of cycles of heating. In the approach described below, the vector lock-in technique is applied simultaneously to the entire video image produced by the IR camera. With this technique the information of each pixel of the image is handled in the manner of a lock-in analyzer, as the object is heated synchronously with the lock-in reference signal. The technique retains the advantage of the IR camera, in that the image is formed essentially in real time, but gains the advantage of lock-in detection, in that the unsynchronous background signal is rejected and the signal-to-noise ratio is enhanced. In effect, one has a lock-in amplifier with a channel for each of the 512 x 512 pixels of the image.

Figure 12 shows a block diagram of this system. The signal from a conventional IR video camera (Inframetrics IR-600) is processed by a video signal processor (manufactured by Datacube, Inc.). The processing consists of digitizing at 10 MHz and digitally merging the video signal with the sine and cosine functions of the phase of the reference signal and accumulating them in separate image buffers (each 512x512x16 bits). When a predetermined number of frames have been accumulated, the results are normalized and displayed as in-phase and quadrature images, in the same manner as the in-phase and quadrature signals are displayed by a vector lock-in analyzer. The postprocessor (a color work-station by Sun Microsystems 3/160C) handles the phase adjustment, pseudocolor and gray scale image display, as well as image storage and retrieval. The phase and timing control assures the synchronization between the heat source and the lock-in analysis. In this arrangement, the lock-in frequency can be chosen from sub-Hz frequencies up to the pixel rate of the IR camera, or the speed of the video signal processing system, whichever is less. For the present system, it is the IR camera speed of about 4 MHz which sets the intrinsic limit of lock-in frequency at about 2 MHz.

[‡]P.K. Kuo, Z.J. Feng, T. Ahmed, L.D. Favro, R.L. Thomas, and J. Hartikainen, Proc. 5th International Topical Meeting on Photoacoustic and Photothermal Phenomena, Springer-Verlag, Heidelberg (to be published).

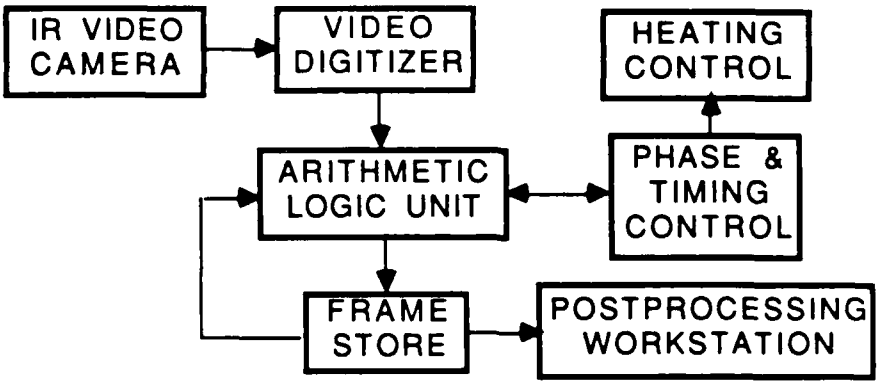

Fig. 12 Block diagram of the vector lock-in IR video imaging system.

To illustrate the principle of area-wide lock-in detection, in Fig. 13a we show a video picture of a circuit board containing an LED display lamp with all its segments turned on by a dc current. Just below it there is another LED, three of whose segments are energized by a weaker current modulated by the reference signal. Figure 13b shows the results of the in-phase image after just two cycles of accumulation. One sees that the only discernable features are the modulated LED segments, all other features having been eliminated by lock-in detection. There is, however, a considerable amount of noise in the background. Increasing the number of cycles of averaging decreases the background noise but keeps the magnitude of the modulated signal the same.

(a) (b)

Fig. 13 A video image of a circuit board (a), together with its lock-in image after just two cycles of averaging (b), illustrating the suppression of non-synchronous features of the image.

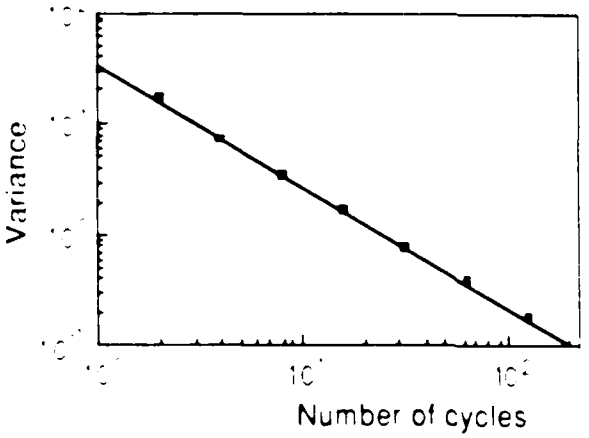

Fig. 14 Plot of the variance of the lock-in image of Fig. 13b as a function of the number of accumulating cycles.

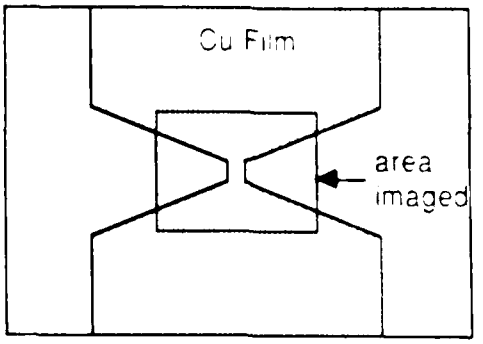

Fig. 15 Schematic diagram of the samples used in Figs. 16 and 17, showing the shape of the copper microbridge.

Figure 14 plots the variance of the images versus the number of averaging cycles. This number plays the same role as the time constant in the conventional lock-in analyzer. The linear relationship shown in Fig. 14 indicates a signal to noise ratio which improves as one over the square root of the

number of averaging cycles, as predicted by theoretical statistical analysis. The simultaneous acquisition of both the in-phase and the quadrature images is of practical importance here because it makes possible the reconstruction of the image of any other required phase from stored image data. With lock-in analysis capability, video thermal wave imaging now enjoys the same advantage as conventional scanned thermal wave imaging, namely, the retention of the phase information contained in the images. Such information can be very useful, for example, in providing characteristic signatures of different types of subsurface defects. [5,6] We have applied this video IR lock-in analyzing system to a sample of laminar structure. The sample consists of a copper film microbridge (a few microns thick) on a polymer substrate, covered by a thin (about 10 μm) film of Kapton [7] as shown in Fig. 15. The microbridge in the copper film provides a convenient means of localized joule heating.

Figures 16a and 16b show the in-phase and quadrature images of this sample when it is being heated by a square-wave current at 15 Hz. Figures 17a and 17b show the same images (taken with the same average input power) of another sample with a simulated debond built into it. The simulated debond was produced by inserting a film of Teflon [8] underneath the microbridge while it is being bonded to the substrate. It is evident that the increased thermal resistance due to the debond causes the ac temperature to increase sharply. It should be pointed out that since copper is a very poor emitter in this wavelength range, the radiation seen in the images comes mainly from the Kapton top layer which is heated by the copper film.

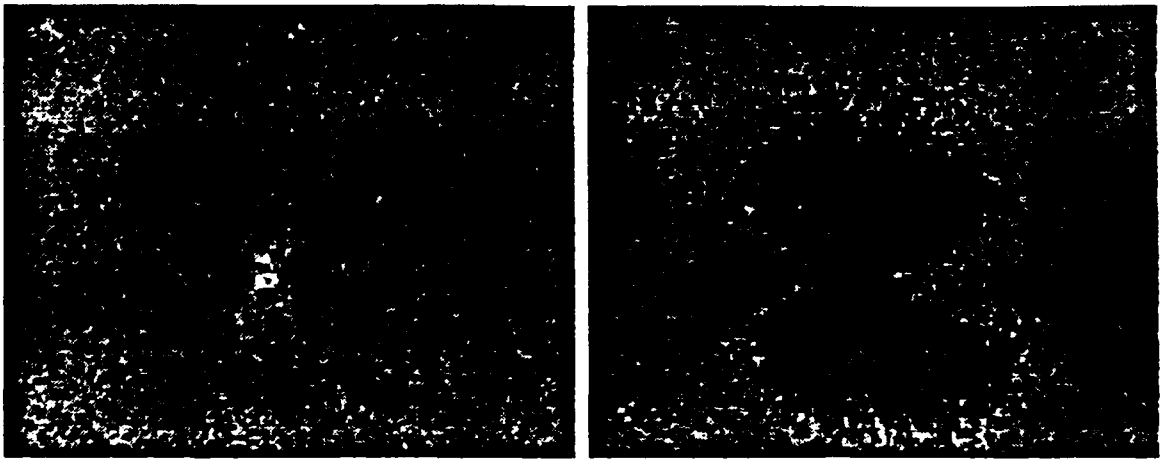

(a) (b)

Fig. 16 In-phase (a) and quadrature (b) lock-in images of a Cu microbridge with no debond.

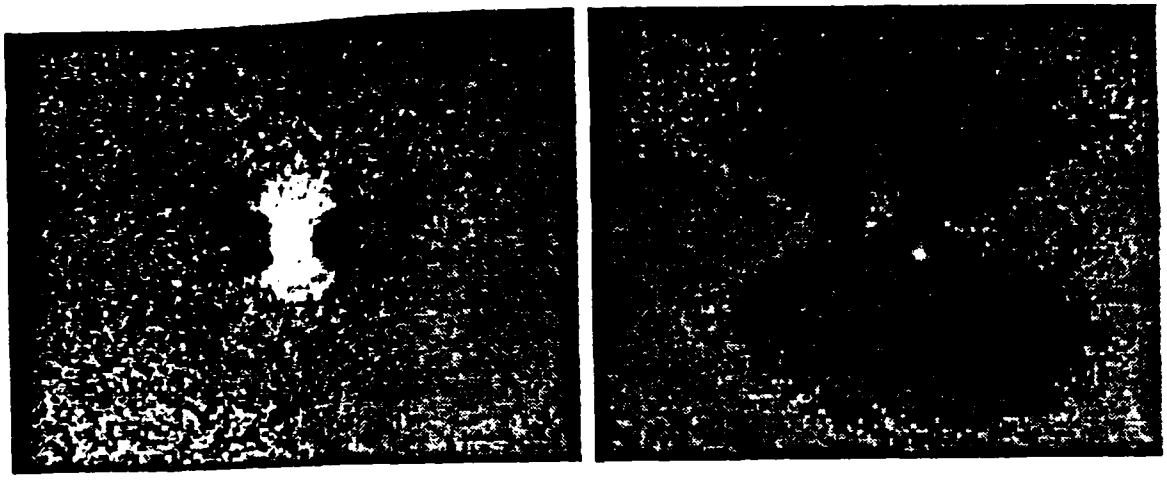

(a) (b)

Fig. 17 In-phase (a) and quadrature (b) lock-in images of a Cu microbridge with a simulated debond. The ac current was adjusted to give the same average power as that used for the Cu microbridge data shown in Fig. 16.

We have also measured samples similar to these, but in which there are microcracks in some of the bridge regions (orientation shown in Fig. 18). A comparison of thermal wave images of two such samples, one without defects, the other containing a microcrack, is given in Figs. 19a and 19b below. These images were taken at a lock-in frequency of 60 Hz. The distortion of the thermal wave pattern caused by the crack is obvious. On the other hand, dc IR images of these bridges do not show any differences between the good and bad samples.

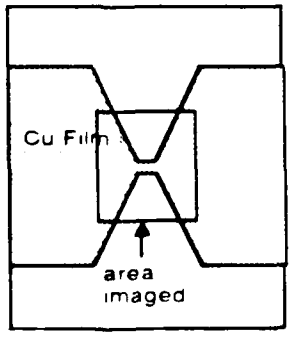

Fig. 18 Orientation of microbridge sample for Images shown in Fig. 19

(a)

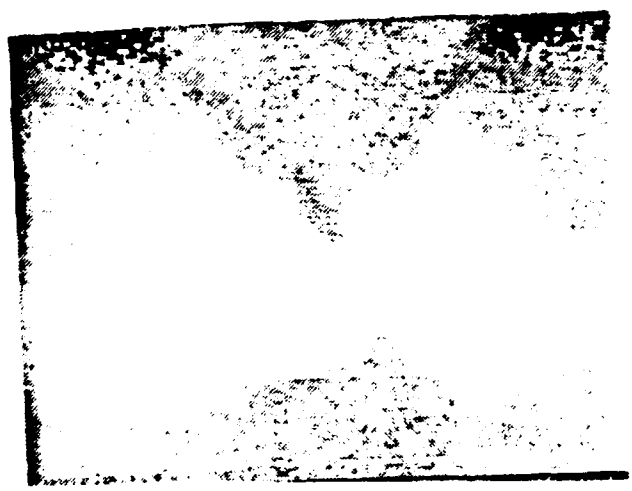

(b)

Fig. 19 Thermal wave IR lock-in images taken at 60Hz of a good Cu microbridge (a), and a Cu microbridge containing cracks (b).

Thermal Wave Imaging Using an Area-Wide Box-Car Averaging Technique[†††]

In this technique the heat source is either a high-energy (up to 5J) flash lamp, coupled by means of an optical light pipe to the sample surface, or a pulse modulated laser (Ar-ion or CO_2). The fast data acquisition hardware and software are used to perform real-time averaging of the entire image field acquired by the IR Video Camera (in transmission or reflection), at a set (variable) time delay following the input of the heat pulse. This method is useful for time scales which typically are long compared to those described for the previous two methods. To illustrate this method, in Fig. 20 we show a transmission image of a Cu/Cu diffusion bond, encapsulated in Kapton, with a thin film of teflon covering one-half of the bond area. This region is easily distinguishable by its cooler temperature as the heat pulse propagates through the region.

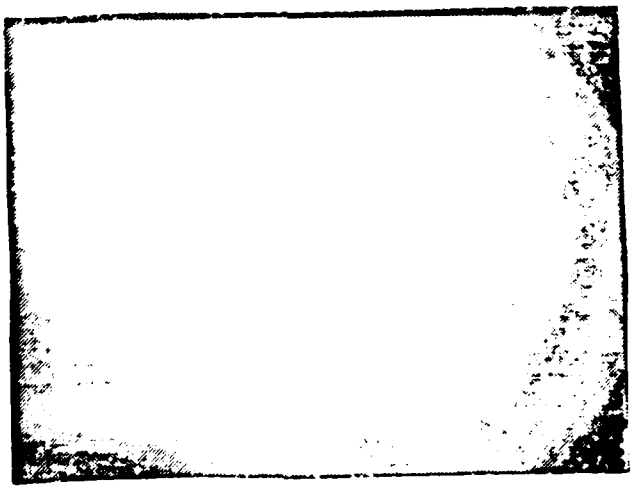

Fig. 20 Transmission image of a Cu/Cu diffusion bond, encapsulated in Kapton, with a thin film of teflon covering one-half of the bond area, using the Area-Wide Box-Car Averaging Thermal Wave Technique. This region is easily distinguishable by its cooler temperature as the heat pulse propagates through the region.

[†††] Unpublished

In Figs. 21 and 22 below, we show thermal wave IR box-car images of a plasma-sprayed coating on the end of a section of a nuclear reactor cooling pipe. In the region imaged there is an area of poor bonding, due to improper substrate surface preparation [in this case, a thin piece of wire lying on the substrate surface was known to have interfered with the sand blasting operation]. Thermal wave images taken at two different time-gate intervals, and are shown in Figs. 21and 22 to illustrate the usefulness of the variable time-gate setting in optimizing the contrast for the subsurface defect of interest. Once again, the dc IR imaging of this region does not detect the defect. It should be noted that these box-car images, like the lock-in images can be obtained very rapidly, and therefore represent an excellent opportunity for development of factory-applicable instrumentation in the near future.

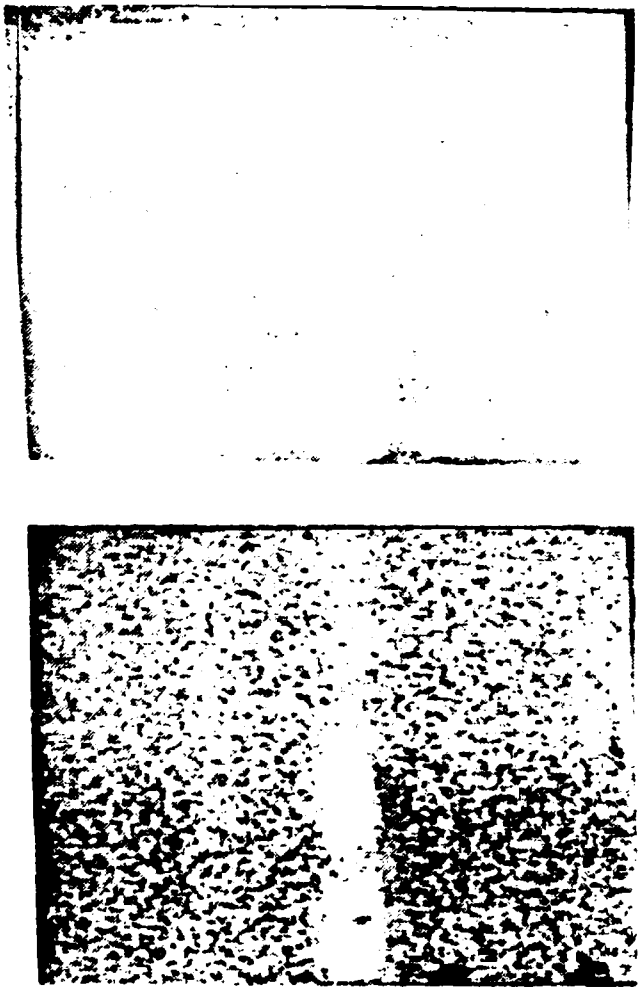

Plasma - sprayed coating on a nuclear reactor cooling pipe

Fig. 21 (t = 67 msec after heating) Fig. 22 (t = 250 msec after heating)

Finally, in Fig. 23 below we show a split image (thermal wave box-car) of two sections of paint panels obtained from an automobile company. The left half of this image is of a panel with known subsurface damage, the right half an image of a nominally undamaged panel. The two panels were placed next to one another and imaged a very short interval following the heating pulse (same pulse for both panels). Thermal evidence for the subsurface damage can be seen on the left half of the image.

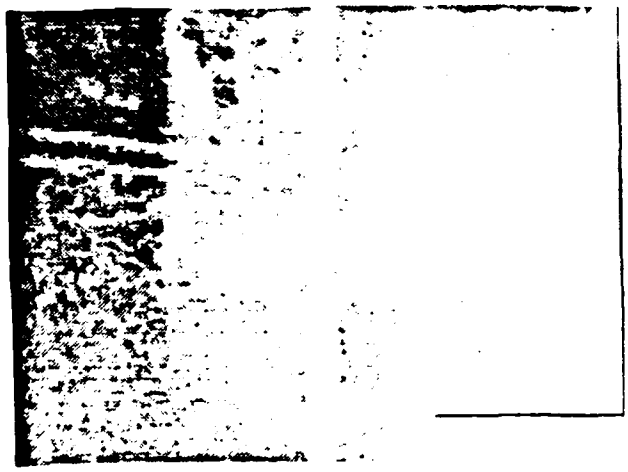

Fig. 23 Thermal image of a good painted metal panel (right) and one with subsurface defects (left).

Theoretical and experimental approaches to the thermoacoustic problem.

The thermoacoustic microscope, which has proven to be useful for the detection of subsurface features on a microscopic scale, has not been fully understood theoretically. In particular, an exact, 3-dimensional solution to the thermoacoustic equations, which form the mathematical basis of the thermoacoustic microscope, had not been found prior to the work carried out during this contract. We have developed an infinite space Green's function for the coupled thermoacoustic equations, using an eigenmode approach. Our approach yielded an exact solution, as opposed to perturbative approaches used by other authors. We have considered in detail the interaction of the infinite space solutions with a boundary surface, and used a matrix formalism to allow the boundary conditions to be expressed as operators. A half-space Green's function was created by operating on the infinite space Green's function with the surface scattering operator. The reflection and mode-conversion of each wave generated by a laser (or particle) source has been described. The far-field angular distributions of the various waves generated by energy and momentum sources have been obtained, and agree with the expected behavior of thermal and acoustic waves in the presence of a boundary.

The significance of the method used here lies in the fact that the thermal wave is put on equal footing with the acoustic waves. This allows the thermoacoustic mode-conversion process to be better understood, and allows one to identify all contributions to the thermoacoustic microscope signal. An expression has been obtained for the thermoacoustic signal corresponding to an aluminum slab with a subsurface crack, and numerical evaluation of the expression is currently in progress.

The corresponding experimental work consisted of the building of a laser heterodyne interferometer to measure the small surface displacement associated with thermal expansion due to periodic heating of a solid. A block diagram of this instrument is given in Fig. 24. The thermal bump generated on a polished aluminum sample was measured with this instrument (see Fig. 25), and was found to have a sensitivity detection limit of 2.2×10^{-4} A$(W/Hz)^{1/2}$, which compares reasonably with that of other instruments reported in the literature.

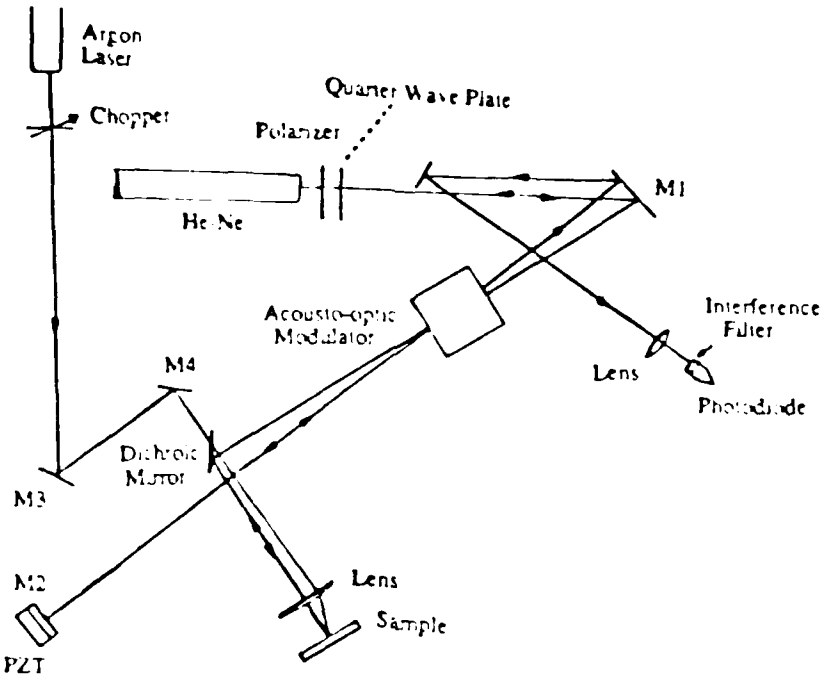

Fig. 24 Block diagram of the laser heterodyne interferometer

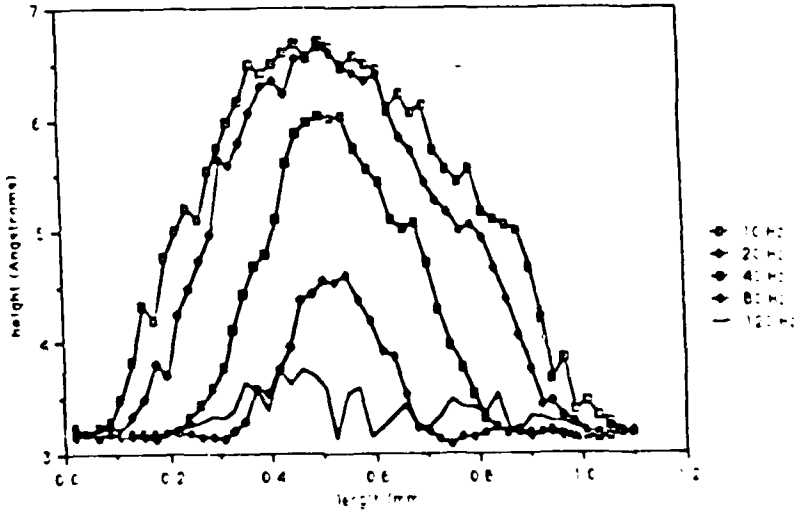

Fig. 25 Line scans of the thermal bump using the laser heterodyne interferometer

C. LIST OF ALL PUBLICATIONS AND TECHNICAL REPORTS

Patent:

U.S. Patent Number 4,589,783: "Thermal Wave Imaging Apparatus", R.L. Thomas, P.K Kuo, and L.D. Favro, May 20, 1986.

Publications:

"Spatial Resolution of Thermal Wave Microscopes", L.J. Inglehart, M.J. Lin, L.D. Favro, P.K. Kuo, and R.L. Thomas, *Proc. 1983 IEEE Ultrasonics Symposium*, edited by B.R. McAvoy (IEEE, New York, 1983), pp. 668-671.

"Thermal Wave Imaging for NDE of Electronic Components", R.L. Thomas, A. Rosencwaig and J. Opsal, *Review of Progress in Quantitative Nondestructive Evaluation*, **Vol. 4B**, D.O. Thompson and D.E. Chimenti, Eds., Plenum (1985), pp. 1177-1188.

"Thermal Wave Detection of Vertical Cracks in Opaque Solids", M.J. Lin, L.J. Inglehart, L.D. Favro, P.K. Kuo and R.L. Thomas, in *Review of Progress in Quantitative Nondestructive Evaluation*, **Vol. 4B**, D.O. Thompson and D.E. Chimenti, Eds., Plenum (1985), pp. 739-744.

"Theory of Mirage Effect Detection of Thermal Waves in Solids", P.K. Kuo, L.J. Inglehart, E.D. Sendler, M.J. Lin, L.D. Favro and R.L. Thomas, in *Review of Progress in Quantitative Nondestructive Evaluation*, **Vol. 4B**, D.O. Thompson and D.E. Chimenti, Eds., Plenum (1985), pp. 745-751.

"Resolution Studies for Thermal Wave Imaging", L.J. Inglehart, D.J. Thomas, M.J. Lin, L.D. Favro, P.K. Kuo and R.L. Thomas, in *Review of Progress in Quantitative Nondestructive Evaluation*, **Vol. 4B**, D.O. Thompson and D.E. Chimenti, Eds., Plenum (1985), pp. 753-759.

"Thermal Wave Imaging for NDE of Metals", Proc. *1984 Metals Congress Session on In-Process* Nondestructive Characterization and Process Control, in the *ASM Metals/Materials Technology Series*, 8408-004 (1984).

"Spatial Resolution of Thermal-Wave and Thermoacoustic Microscopes", L.D. Favro, P.K. Kuo and R.L. Thomas, in *Acoustical Imaging*, **Vol. 14**, Ed. by A.J. Berkhout, J. Ridder, and L.F. van der Wal (Plenum, 1985), pp. 361-365.

"Thermal Wave Imaging of Defects in Opaque Solids," D.N. Rose, D.C. Bryk, D.J. Thomas, R.L. Thomas, L.D. Favro, P.K. Kuo, L.J. Inglehart, M.J. Lin, and K.O. Legg, in *Advances in Materials Characterization II*, Ed. R.L. Snyder, R.A. Condrate, Sr., and P.F. Johnson, Materials Science Research, **Vol. 19**, pp. 221-239, Plenum (1985).

"Thermal Wave Imaging for NDE", R.L. Thomas, L.D. Favro, and P.K. Kuo, *Can. J. Phys.* **64**, 1234 (1986).

"Mirage Effect Measurement of Thermal Diffusivity, Part I - Experimental", P.K. Kuo, M.J. Lin, C.B. Reyes, L.D. Favro, R.L. Thomas, D.S. Kim, S.Y. Zhang, L.J. Inglehart, D.Fournier, A.C. Boccara and N. Yacoubi, *Can. J. Phys*. **64**, 1165 (1986).

"Mirage Effect Measurement of Thermal Diffusivity, Part II - Theory", P.K. Kuo, E.D. Sendler, L.D. Favro, and R.L. Thomas, *Can. J. Phys*. **64**, 1168 (1986).

"Contrast Mechanisms in the Thermoacoustic Microscope", L.D. Favro, P.K. Kuo, and R.L. Thomas, in *Review of Progress in Quantitative NDE*, **Vol. 5A**, D.O. Thompson and D.E. Chimenti, Eds., Plenum (1986) pp. 439-445.

71. "Thermal Wave Imaging of Defects in Opaque Solids," D.N. Rose, D.C. Bryk, D.J. Thomas,

R.L. Thomas, L.D. Favro, P.K. Kuo, L.J. Inglehart, M.J. Lin, and K.O. Legg, in Materials Characterization for Systems Performance and Reliability, Eds. J.W. MacCauley and V. Weiss, *Sagamore Army Materials Research Conference Procs.*, Vol. 31, pp. 547-564, Plenum (1986).

"Thermal Wave Imaging for Quantitative Nondestructive Evaluation," R.L. Thomas, L.D. Favro, and P.K. Kuo, *Proc. ONR Symposium on Solid Mechanics Research for QNDE*, Ed. by J.D. Achenbach and Y. Rajapakse (Martinus Nijhoff, Boston, 1986), pp. 239-253.

"Reflection-Mirage Measurements of Thermal Diffusivity", C.B. Reyes, J. Jaarinen, L.D. Favro, P.K. Kuo, and R.L. Thomas, *Review of Progress in Quantitative NDE*, Vol. 6, edited by D.O. Thompson and D. Chimenti, Plenum New York (1987), pp. 271-275.

"Thermal Wave Techniques for Imaging and Characterization of Materials", L.D. Favro, P.K. Kuo, and R.L. Thomas, *Review of Progress in Quantitative NDE*, Vol. 6, edited by D.O. Thompson and D. Chimenti, Plenum New York (1987), pp. 293-299.

"Sound Generation in a Thermoacoustic Microscope", L.D. Favro, P.K. Kuo, S.M. Shepard and R.L. Thomas, *Proc. 1986 IEEE Ultrasonics Symposium*, edited by B.R. McAvoy (IEEE, New York, 1986), pp. 399-482.

"Thermal Wave Propagation and Scattering in Semiconductors", R.L. Thomas, L.D. Favro, and P.K. Kuo, in *Photoacoustic and Thermal Wave Phenomena in Semiconductors*, ed. A. Mandelis, Elsevier, New York (in press).

"Photothermal Deflection (mirage) Detection of Diffusivities and Surface and Subsurface Defects in Solids", P.K. Kuo, L.D. Favro, and R.L. Thomas, in *Photothermal Deflection Spectroscopy and Applications"*, ed. J.A. Sell, Academic Press (in press).

"Mechanisms for the Generation and Scattering of Sound and Thermal Waves in Thermoacoustic Microscopes", L.D. Favro, S.M. Shepard, P.K. Kuo, and R.L. Thomas, Invited paper, *Proc. 5th International Topical Meeting on Photoacoustic, Thermal and Related Sciences, Heidelberg, July 27-30, 1987* (Springer-Verlag, to be Published).

"Time-Resolved IR Video Imaging with Synchronized Scanned Laser Heating", P.K. Kuo, I. C. Oppenheim, L.D. Favro, Z.J. Feng, R.L. Thomas,J. Hartikainen, and L.J. Inglehart, *Proc. 5th International Topical Meeting on Photoacoustic, Thermal and Related Sciences, Heidelberg, July 27-30, 1987* (Springer-Verlag, to be Published).

"Sound Production Mechanisms in Thermoacoustic Microscopes", invited paper, L.D. Favro, S.M. Shepard, P.K. Kuo, and R.L. Thomas, *Review of Progress in Quantitative NDE*, Vol. 7, edited by D.O. Thompson and D. Chimenti, Plenum New York (to be published).

"Parallel Thermal Wave Imaging Using a Vector Lock-In Video Technique, *Proc. 5th International Topical Meeting on Photoacoustic, Thermal and Related Sciences, Heidelberg, July 27-30, 1987* (Springer-Verlag, to be Published).

"Optical/Thermal Wave Techniques for Thin-Film Metrology", P.K. Kuo, R.L. Thomas, and L.D. Favro, *Proc. International Conf. on Photomechanics and Speckle Metrology, SPIE, San Diego, August 17-20, 1987, SPIE Proceedings Vol. 814 (1987).*

"Measurement of Opaque Film Thickness", R.L. Thomas, J. Jaarinen, C. Reyes, I.C. Oppenheim, L.D. Favro, and P.K. Kuo, in *Electronics Reliability and Measurement Technology, Proc. NASA Langley Research Center Conference, June 3-5, 1986, NASA Conf. Publication 2472 (1987), pp. 73-83 (1987).*

"Thermal Wave Microscopy", R.L. Thomas, L.D. Favro and P.K. Kuo, *Proc. 11th Triennial World Congress of the International Measurement Confederation* (in preparation).

Reports:

In addition to the regular semi-annual progress reports, the following letter reports have been made:

June 19, 1987 - Letter progress report to Dr. Wilbur Simmons, describing recent IR thermal wave imaging work which was to be presented at the Williamsburg NDE meeting and the Heidelberg Photoacoustics meeting.

August 14, 1987 - Letter progress report to Dr. Iqbal Ahmad, describing a few highlights of our accomplishments during the contract period to that time, with special emphasis on the developments which were made possible as the result of the ARO Instrumentation Grant (DAAL03-86-G-0169). [The Final Technical Report for that Grant was submitted August 19, 1987].

September 28, 1987 - A more extensive letter progress report to Dr. Iqbal Ahmad, providing highlights of all ARO-sponsored research in thermal wave imaging and characterization since its inception at WSU.

D. LIST OF ALL PARTICIPATING SCIENTIFIC PERSONNEL AND ADVANCED DEGREES EARNED WHILE EMPLOYED ON THE PROJECT

Professor L. D. Favro, Co-Principal Investigator

Professor P.K. Kuo, Co-Principal Investigator

Professor R.L. Thomas, Co-Principal Investigator

Professor Ming-Juei Lin, Visiting Professor

Professor Shu-Yi Zhang, Visiting Professor

Dr. Tasdiq Ahmed, Research Associate

Mr. Z.J. Feng, Visiting Scholar

Mr. Jari Hartikainen, Visiting Scholar

Mr. Jussi Jaarinen, Visiting Scholar

Mr. H. Jin, Visiting Scholar
Ms. Celeste B. Reyes, Graduate Assistant (Ph.D. Dissertation, "Thermal Wave Measurement of Thermal Diffusivities of Solids", expected completion date: January, 1988).

Mr. Steven M. Shepard, Graduate Assistant (Ph.D. Dissertation, "Theoretical and Experimental Approaches to the Thermoacoustic Problem", expected completion date: November, 1987).

Mr. Mahendra Munidasa, Graduate Assistant (Ph.D. candidate, expected completion date: December, 1988).

Mr. Yiqian Wang, Graduate Assistant (Ph.D. candidate, expected completion date: June, 1989).

Mr. Yanan Li, Graduate Assistant (M.S., "An Investigation of True Temperature Measurement with Infrared Techniques": January, 1987).

Mr. Tianxiao Li, Graduate Assistant (M.A., February, 1987).

Ms. Ping Chen, Graduate Assistant (M.S. candidate, expected completion date: June, 1987).

Mr. Kyle Simon, Skillman Fellow (M.S. candidate, expected completion date: June, 1987).

Ms. Peggy Talley, Graduate Assistant (M.S. candidate, expected completion date: June, 1988)

BIBLIOGRAPHY

1. W.N. Reynolds: In Can. J. Phys. **64**, 1150 (1986).

2. D.M.Heath, C.S. Welch, W.P. Winfree, J.S. Heyman, and W.E. Miller: In Review of Progress in Quantitative Nondestructive Evaluation, D.O. Thompson and D.E. Chimenti, Eds., Vol. **5B**, 1125 Plenum, New York (1986).

3. C.S. Welch, D.M.Heath, and W.P. Winfree: In Review of Progress in Quantitative Nondestructive Evaluation, D.O. Thompson and D.E. Chimenti, Eds., Vol. **5B**, 1133 Plenum, New York (1986).

4. L.J. Inglehart, K.R. Grice, L.D. Favro, P.K. Kuo, and R.L. Thomas, Appl. Phys. Lett. **43**, 446 (1983).

5. K.R. Grice, L.J. Inglehart, L.D. Favro, P.K. Kuo, and R.L. Thomas, J. Appl. Phys. **54**, 6245 (1983).

6. P.K. Kuo, L.D. Favro, L.J. Inglehart, and R.L. Thomas, J. Appl. Phys. **53**, 1258 (1983).

7. Polyimide film, reg. U.S. Patent Office, E.I. du Pont Nemours and Co., Inc.

8. Tetrafluoroethylene film, reg. U.S. Patent Office, E.I. du Pont Nemours and Co., Inc.